Available online at www.sciencedirect.com
SCIENCE DIRECT®
ELSEVIER
Microelectronic Engineering 69 (2003) 118–129
MICROELECTRONIC ENGINEERING
www.elsevier.com/locate/mee

The role of localized states in the degradation of thin gate oxides

Gennadi Bersuker[a,*], Anatoli Korkin[b], Leonardo Fonseca[b], Andrey Safonov[b], Alexander Bagatur'yants[b], Howard R. Huff[a]

[a]*International SEMATECH, 2706 Montopolis Dr., Austin, TX 78741, USA*
[b]*DigitalDNA Labs Semiconductor Products Sector, Motorola Inc., 2100 E. Elliot Road, MD EL722, Tempe, AZ 85202, USA*

Abstract

A model is proposed to address the effects of oxide electric field and anode bias, as well as the role of hydrogen, in the trap generation process. The oxide wear-out phenomenon is considered as a multi-step process initiated by the capture of injected electrons by localized states in SiO_2. The captured electrons significantly weaken the corresponding Si–O bond, which becomes unstable with respect to the applied electric field and temperature. The hydrogen present in the oxide (due to the anode hydrogen release process) prevents restoration of the broken bonds and leads to the generation of neutral E′ centers. The model describes the charge-to-breakdown dependence on the electron energy, electric field, temperature, and oxide thickness.

Keywords: Silicon dioxide; Gate oxide; Wear-out; Breakdown; Reliability; Atomistic model

1. Introduction

Degradation of gate oxides under electrical stress has long been seen as caused by the trap generation phenomenon [1,2], although the nature of the traps remains unclear. One may expect the concurrent creation of several types of traps associated with different physical processes that simultaneously take place during stress, while only one of them might be the primary cause of the oxide breakdown under the given stress condition. Even in the case of structurally identical traps, a wide range distribution of the trap energies (for instance, due to elastic and/or electrical interaction between closely located traps) may translate into a variation of the electrical properties of the traps. As an indication of the variety of oxide trap electrical properties, one may consider the following: the traps causing stress induced leakage current (SILC) demonstrate different annealing kinetics and time scale of generation from the ones responsible for breakdown [3,4], and both types of traps are generated by the constant voltage stress (CVS) procedure. On the other hand, traps generated by two different methods, hot hole injection and CVS, cause different breakdown defect density and temperature dependence [5,6] (see Discussion).

Recent electron spin resonance (ESR) data point to active E′ centers, which consist of a three-coordinated Si atom with an unpaired electron, as the most likely defect responsible for electrical degradation of stressed oxide films [7]. In principle, an E′ center can be formed as the result of the breakage of an O–Si bond or a bond associated with an oxygen vacancy, such as a Si–Si bond. The latter have attracted primary attention since weak Si–Si bonds can be broken by either an external electric field or

*Corresponding author.
E-mail address: gennadi.bersuker@sematech.org (G. Bersuker).

0167-9317/03/$ – see front matter
doi:10.1016/S0167-9317(03)00288-0

by reactions with hydrogen or holes, corresponding to the electrochemical [8], hydrogen release [9], and anode hole injection [10] oxide degradation models, respectively. In this case, oxygen vacancies represent precursor breakdown defects whose initial (before the stress) distribution in the oxide pre-determine the possible location and density of E′ centers. The O–Si bonds, being too strong to be broken by any of the above mechanisms, have not being considered as a potential source of E′ centers.

However, the interaction between the oxide bonds and injected electrons may open chemical pathways for breaking Si–O bonds more easily. Indeed, the tunneling approximation usually employed to describe electron transport through thin oxides under low bias conditions fails for injected electrons passing near localized states in the SiO_2 band gap [11]. These states can be generated by irregularities/structural defects in the oxide. In particular, localized states can be induced by SiO_2 bond distortions caused by the nearby O-vacancies and/or broken Si–O bonds. The increase of the average O–O nearest neighbors distance due to missing or displaced O atoms has been shown to result in the formation of localized states associated with the oxygen p-states split-off from the bottom of the SiO_2 conduction band [12]. The density of localized states also increases significantly near the Si/SiO_2 interface, where a strained transition layer characterized by O-deficiency [13–15], is formed in the oxide to accommodate the atomic mismatch between SiO_2 and the silicon substrate.

Localized states can capture injected electrons if the energies of the former and the latter are in resonance. We shall describe how such electron capture triggers the chain of events leading to a Si–O bond breakdown and eventually E′ center generation. We then qualitatively discuss the consequences of the proposed model regarding the formation of a conductive path and its subsequent degradation that causes the dielectric breakdown.

2. Modeling oxide structural conformations

Recently we have proposed an atomistic model of defect generation in silicon oxide gate dielectrics [15,16]. The model is based on the assumption that an electron captured at a localized level in the gap may cause breaking of the Si–O bond. We start by investigating how the electron capture by the localized state affects the Si–O–Si bond.

In order to model the effects of an electron attachment, a simple cluster type model based on the molecule $F_3SiOSiF_3$, which contains a Si–O–Si 'reaction center' was used. The fluorine termination was employed since it better emulates the electric charge on a silicon atom in an oxide than hydrogen termination. Quantum-chemical computations of this cluster were performed [17] using two density functional theory (DFT) methods, the local spin density approximation (LSDA SVWN5) and the hybrid Becke–Lee–Yang–Parr functional (B3LYP), as well as the ab initio Moller–Plesset second order perturbation theory (MP2) [18] implemented in the Gaussian 98 program [19]. We used a 3−21G basis set in LSDA and a 6−31G basis set in B3LYP and in MP2 calculations augmented by diffuse s and p and polarization d functions (e.g. 3−21+G* and 6−31+G*).

The captured electron was found to preferentially reside on the anti-bonding orbital resulting in a dramatic energy reduction, on the order of 75%, of the Si–O bond (compare the first two rows in Table 1). This weakened, negatively charged Si–O bond with a trapped electron (Fig. 1a) represents a precursor breakdown defect since it is shown to be unstable with respect to an external electric field and temperatures typically used in stress measurements (see next section). Breakdown of this bond leads to the creation of a neutral defect center, a three-coordinated Si+non-bridging O (NBO), when the captured electron leaves the oxygen:

Table 1
Electron capture effect on bond energies (in kcal/mol) of the model species containing a Si–O–Si 'reaction center' calculated by SVWN5 and B3LYP DFT, and ab initio MP2 methods[a]

Model reaction	SVWN5	B3LYP	MP2
$F_3SiOSiF_3 \rightarrow F_3Si + OSiF_3$	164.2	134.0	145.4
$F_3Si{-}OSiF_3^- \rightarrow F_3Si + OSiF_3^-$	63.0	39.0	38.9
$F_4Si{-}OSiF_3^- \rightarrow F_4Si + OSiF_3^-$	64.1	37.8	39.0

[a] The calculated energies are semi-quantitative estimates. In order to get accurate values highly correlated methods, e.g. coupled cluster theory and much larger basis sets, have to be used in the computations.

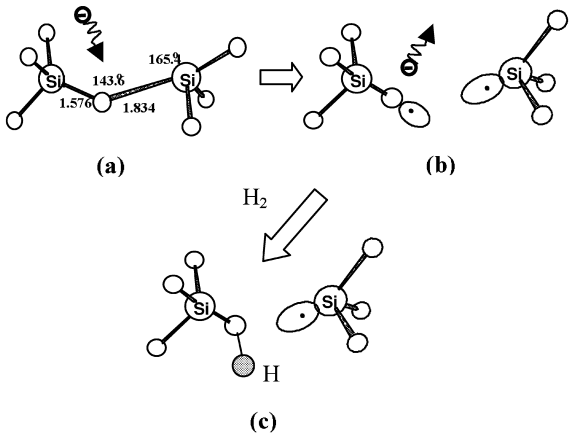

Fig. 1. Schematics of the proposed E′ center generation process.

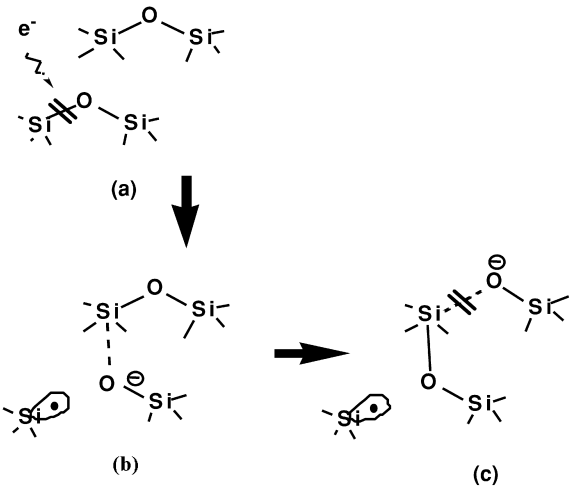

Fig. 2. A model for the E′ center generation and structural relaxation in SiO_2 triggered by an electron capture. (a) Electron capture followed by the breaking of the weakened Si–O bond; (b) the case of a long electron lifetime on a non-bridging oxygen: formation of a donor–acceptor bond between the negatively charged O and a neighboring Si; (c) subsequent migration of the negative charge via bond breaking–swapping resulting in a stable E′ center.

$$\equiv Si{-}O{-}Si\equiv + e \rightarrow \equiv Si{-}O^{-}{-}Si\equiv \xrightarrow{E_{ox},T} \equiv Si{-}O^{\bullet} + {}^{\bullet}Si\equiv + e \quad (1)$$

where $O^{\bullet}$ and ${}^{\bullet}Si$ represent O and Si with an unpaired electron, respectively, $\equiv Si$ denotes Si bonded to three oxygen atoms, and e is a free electron (Fig. 1b).

As follows, an electron capture by the Si–O–Si bond, which is weakened by stress, as is characteristic for the Si/SiO_2 interface [20], may lead to the Si–O bond breakage without an electric field applied, as was observed in hot carrier injection experiments [21].

If the captured electron is released before any major structure relaxation takes place, the broken Si . . . O bond can be reconstructed by high temperature anneal. However, hydrogen, if present in the oxide, may prevent annealing of the defect center, as shown in Fig. 1c. Calculations show that the reaction of H_2 with NBO is exothermic with an energy gain of 0.40 eV [22] (while a similar reaction involving Si is endothermic) resulting in the formation of a neutral E′ center:

$$\equiv Si{-}O^{\bullet} + {}^{\bullet}Si\equiv + H_2 \rightarrow \equiv Si{-}OH + {}^{\bullet}Si\equiv + H \quad (2)$$

If the lifetime of the captured electron on the dangling oxygen is long enough, a donor–acceptor bond could be formed between the negatively charged oxygen and neighboring Si, as shown in Fig. 2 [17]. Indeed, the donor–acceptor Si–O bond connecting the SiF_4 complex and $OSiF_3^-$ anion has about the same energy as the Si–O bond in the $F_3Si{-}OSiF_3^-$ anion (compare the 2nd and 3rd rows in Table 1), and the donor–acceptor Si–O bond in the $F_4Si{-}OSiF_3^-$ complex (1.774 Å) is shorter than the corresponding bond in the $F_3Si{-}OSiF_3^-$ anion (1.834 Å). We speculate that if steric factors allow (in particular, the presence of two Si atoms located in close proximity in the amorphous SiO_2 network), the captured electrons may then migrate via the Si–O network to the next-neighbor oxygen (see Fig. 2) causing the rearrangement of the Si–O bond network and leaving behind a E′ center. Our calculations (see [17] for details) show that the barrier for the 'Si–O^- defect' migration can be small. This electron migration via bond breaking–swapping may continue until the electron is released and the above mentioned reaction between the dangling O and molecular hydrogen 'locks' the dangling oxygen through the formation of an O–H bond.

In order to investigate the energetics of the defect proposed in Reaction (2) more realistically, we compared the total energy of α-quartz-SiO_2 containing the 'Si–OH + Si˙' defect (see Fig. 3) with

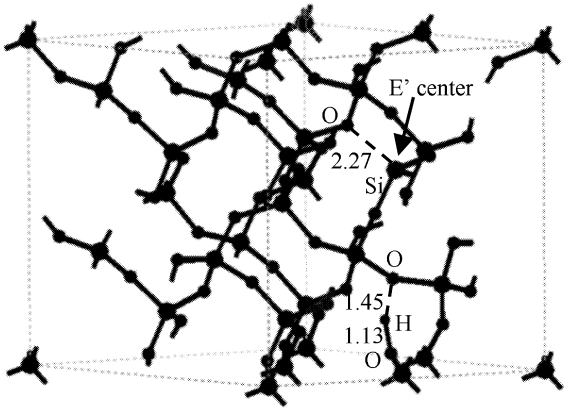

Fig. 3. Unit cell used in the periodic calculations of the energetics of the E′ center. The distances of the closest neighbors to the E′ center and H interstitial after ionic relaxation are indicated.

α-quartz-SiO_2 containing a hydrogen interstitial. All calculations were performed using the local-density approximation (LDA) [23] within density-functional theory (DFT) [24] as implemented in the pseudo-atomic local orbital SIESTA code [25]. The electronic ground state was determined self-consistently using the preconditioned conjugate gradient method [26] through the solution of the Kohn–Sham equations, and the ionic positions were optimized to minimize the Hellmann–Feynman forces [27]. Norm-conserving non-local pseudopotentials of the Troullier–Martins type [28] were used to describe all the elements considered. A 72-atom unit cell was used to minimize the interaction between the periodic dangling bonds. Forty-eight special k-points were used to sample the irreducible wedge of the Brillouin zone. The structures were relaxed using a single-ζ (SZ) basis set and the total energies of the relaxed structures were calculated with SZ and double-ζ plus polarization (DZP) bases sets to check for the convergence of the energy difference between the two structures, the one with the E′ center (see Fig. 3) and the regular α-quartz-SiO_2 structure with an interstitial hydrogen atom. The molecular model of the 'Si–OH + Si' defect shown in Fig. 3 was generated from the following steps: (1) breaking a single Si–O bond; (2) rearranging the bonding to separate the Si–$O^{\cdot}$ and $Si^{\cdot}$ dangling bonds (according to the process illustrated in Fig. 2); (3) stabilizing the oxygen defect by formation of an O–H bond; and (4) relaxing the new structure.

Our periodic boundary calculations show that the '*defective form*' (see Fig. 3), which includes the E′ center, is 4.1 eV *more stable* than the *ideal* α-quartz structure with an interstitial hydrogen in it. We found that this result changes negligibly with different calculation basis sets. This finding supports the concept of hydrogen acting as a 'locking' factor and the following stabilization of the E′ center. The three-coordinated silicon atom, which forms the E′ center, is at a short (2.27 Å) distance to the closest oxygen atom, while the OH group forms a hydrogen bond with the neighboring oxygen.

The density of state (DOS) of two structures is shown in Fig. 4 and compared to the ideal α-quartz case. The structure that contains the interstitial hydrogen atom has a DOS very similar to the ideal case (except for the extra H gap state), while the structure which contains the Si–OH and the three coordinated silicon (E′ center) reveals a striking difference from the ideal alpha-quartz, namely a large density of states below the conduction band edge. The localized states, which appeared in the middle of band gap, result from non-paired electrons localized either on silicon (E′ center) or on the interstitial hydrogen.

3. Electron trap generation in bulk oxide

Based on the above model for electron trap generation in the bulk oxide caused by the capture of injected electrons by localized states (oxygen antibonding states), we derived an expression that describes the dependence of the bond breakdown probability, which is assumed to be proportional to the charge-to-breakdown, on oxide thickness, stress bias, temperature, and energy of the injected electrons [15,16].

Considering a thin oxide, where the oxide thickness is comparable to the electron mean free path, the probability of electron capture by localized states over the electron travel distance t from the cathode can be approximated by the following expression, which is analogous to the absorption coefficient:

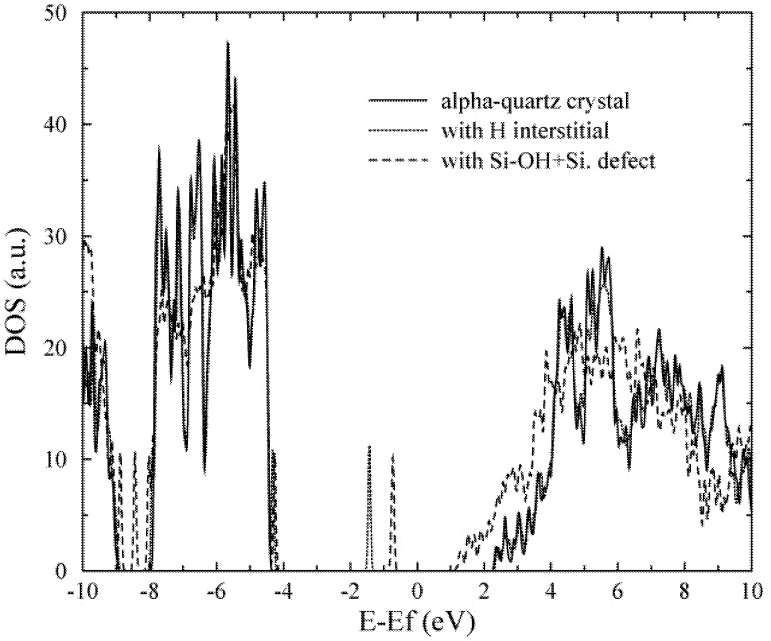

Fig. 4. Density of states of the ideal α-quartz crystal, α-quartz with the Si–OH + Si· defect, and α-quartz with a hydrogen interstitial.

$$K = 1 - \exp(-st) \tag{3}$$

where s is the electron mean free path in SiO_2. The probability of electron capture by a localized state at t is proportional to the probability of the electron-state collision, $\partial K/\partial t$, and the density of localized states, $g(E,t)$, where E is the localized state energy measured from the valence band edge. For the sake of simplicity, we assume that the localized states are uniformly distributed through the total oxide thickness (actually, the localized state density increases significantly within the strained transitional layer near the Si/SiO_2 interface [12,14]). Since the localized states are split off from the conduction band of SiO_2 (presumably unoccupied P-states of oxygen [12]), their density is expected to increase towards the bottom of the conduction band. Based on this observation, we approximate $g(E,t)$ by a linear function of the electron kinetic energy, $E_{el} = E_{ox}t$, measured from the valence-band edge. In this case one can derive the following expression for the probability of generation of a precursor defect per injected electron (the probability of electron capture that leads to the generation of an elongated Si–O bond, Fig. 1a):

$$P_F \propto \int_0^{t_0} g(E,t)\frac{\partial K}{\partial t}\partial t \propto \int_0^{t_0} E_{el}(t)\frac{\partial K}{\partial t}\mathrm{d}t = \frac{E_{ox}}{s} \times \left[1 - (1 + st_{ox})\,\mathrm{e}^{-st_{ox}}\right] \tag{4}$$

The explicit dependence on E_{ox} and t in Eq. (4) may change if a different expression for $g(E,t)$ is used, however, the general trend of increasing P_F with the electron energy remains.

The dependence of the bond energy on the bond length (or angle) is schematically illustrated in Fig. 5. The location of the bond energy minimum defines the equilibrium atomic configuration. As discussed in the previous section, in the case where the precursor breakdown defect forms as a result of electron capture, the defect bond is an elongated Si–O bond (Fig. 1a) and the intrinsic bond energy E_0 (curve 1 in Fig. 5) is reduced to $E_a \approx 0.25\,E_0$ (curve 2 in Fig. 5, not to scale).

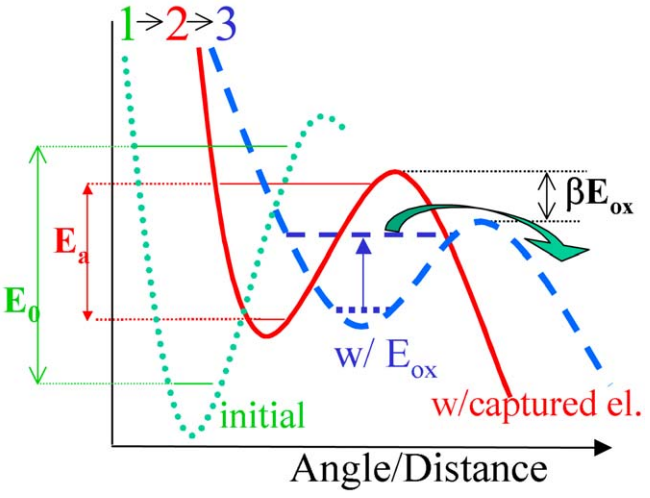

Fig. 5. Schematics of the Si–O bond energy (dotted line, curve 1) change with the capture of an electron (solid line, curve 2) and with applied external electric field and temperature (broken line, curve 3).

The applied electric field shifts the relative positions of the ions and electrons in a bond, thus modifying the bond length. This results in a shift in the position of the potential energy minimum, which becomes shallower, decreasing the bond energy (curve 3 in Fig. 5). In the case of a simple ionic bond within the harmonic oscillator approximation, the change in the barrier height, ΔE, is given by $\Delta E = q\chi E_{ox} \equiv \beta E_{ox}$, where q is the effective ion charge, χ is the change in interatomic distance, and E_{ox} is the electric field component acting parallel to the bond. A detailed analysis of polarization effects in SiO_2 is described by McPherson and Mogul [29] where it is shown that the local electric field acting on a bond may be up to two times higher than the externally applied field (see Fig. 5).

Temperature is associated with the population of excited vibrational states in the potential energy well and the distribution of atomic vibration amplitudes (curve 3 in Fig. 5). If the temperature is increased to sufficient values that the energy states near the top of the well are populated, then the atomic displacements become so large that bonds start to break. The temperature population of vibrational states can be described by the Boltzmann expression, $P \propto \exp(-E_a/kT)$. Thus, in the presence of an external electric field the bond breaking probability takes the form:

$$P_E \propto e^{-(E_a-\beta E_{ox})/kT} \tag{5}$$

where β includes the contribution of the bond polarization to the local electric field [29].

The number N of broken Si–O bonds per unit area, described by Eq. (1), is then given by the expression $N \propto QP_EP_F$, where Q is the total electron current and P_EP_F is the probability of bond breakage per injected electron. According to percolation theory, oxide breakdown occurs when the density of traps (which we assume to be proportional to the density of broken bonds N) reaches some characteristic critical value N_{bd} [30]. The associated critical Q value is called the charge-to-breakdown Q_{bd}. Taking into account that N_{bd} scales with the oxide thickness [30], and using the above expression for N, we obtain:

$$Q_{bd} = \frac{e^{-(\beta E_{ox}-E_a)/kT}}{E_{ox}} \frac{At_{ox}^2}{1-(1+st_{ox})\exp(-st_{ox})} \tag{6}$$

where the constant A includes the proportionality constant between the numbers of broken bonds and stable E′ defects (controlled by the hydrogen supply, Eq. (2)—see Discussion), as well as a contribution from statistical factors not discussed here, in particular the area dependence. The relation between Q_{bd} and E_{ox} deviates from the Arrhenius relation due to the dependence of the precursor defect generation

on the electron kinetic energy (since the latter affects the availability of the localized states in resonance with the injected electron). The bond breaking probability $P_E P_F$ is a weak function of t_{ox}, and the Q_{bd} thickness dependence mostly comes from the N_{bd} parameter [31]. Eq. (6) accounts only for the stress generated traps; the presence of a significant amount of the pre-existing defects in the oxide would require some modification of this equation [15].

As follows from the above discussion, the proposed trap generation mechanism should be more effective in the case of (a) thin oxides where the intrinsically defective transitional layer at the SiO_2/Si interface comprises a significant portion of the total oxide thickness; and (b) low stress voltages when the electron transport through the gate dielectric occurs in the direct tunneling regime.

4. Electrical stress: charge-to-breakdown

Positive and negative constant voltage stresses were performed on n^+ poly capacitors and transistors with areas of 1×10^{-3} cm^2 and 4×10^{-6} cm^2 fabricated on p-type substrates with thermally grown SiO_2 in the range of 2.5–6.5 nm. Different stress voltages and temperatures ranging from 25 to 100 °C were used. The oxide physical thicknesses were verified by C–V measurements taking into account quantum corrections and poly depletion. Special attention was devoted to avoid the series resistance effect in large area capacitors. The first breakdown event, either soft or hard, was considered as the oxide breakdown. The values of the β parameter and bond energy of the precursor defects E_a (see Fig. 6) extracted from the measured Q_{bd} data using Eq. (6) agree qualitatively with previous estimates [29,32], as well as simulation results [17].

The Q_{bd} values were then calculated for large and small area devices as shown in Figs. 7 and 8, respectively, for different E_{ox} using Eq. (6). The best fit between the calculated and measured Q_{bd} values was obtained taking the electron mean free path value, $1/s$, to be about 1.36 nm, in rather good agreement with the value of 1.5 nm estimated by Schuegraf et al. [33]. The mismatch in the two splits is caused by the variation of the proportionality constant A attributed to specific defect/stress distributions in the analyzed devices. The trap generation rate calculated with the critical defect density value as an adjustable parameter and its comparison with previously reported data [34] are shown in Fig. 9.

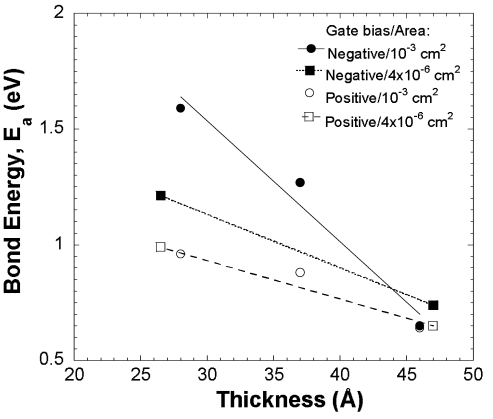

Fig. 6. Dependence of the precursor defect averaged bond energy with the oxide thickness.

The increase of the averaged (over the film thickness) precursor breakdown defect bond energy E_a, as well as the differences between the positive and negative bias E_a values, with the decrease of the oxide thickness may be attributed to the presence of a transition layer at the SiO_2/Si interface [35]. Indeed, according to the proposed model, in the tunneling regime a larger portion of the precursor

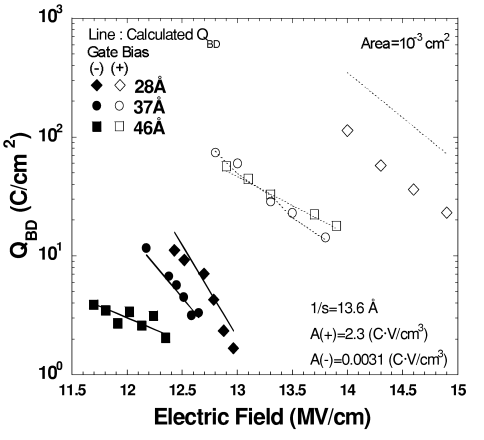

Fig. 7. Q_{bd} values for large area devices—calculated (lines) and measured with positive (open, +) and negative (closed, −) gate bias.

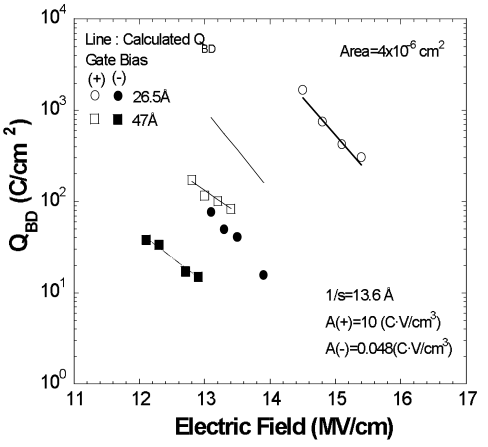

Fig. 8. Q_{bd} values for small area devices—calculated (lines) and measured with positive (open, +) and negative (closed, −) gate bias.

defects tends to be generated at a larger distance from the cathode where the energy of the injected electrons approaches the energy of the oxide conduction band. This effect takes place because the density of localized states in the band gap is known to increase toward the bottom of the conduction band [12]. Therefore, in the case of gate injection, a larger portion of the bond breakage (as compared to the case of substrate injection) occurs within the oxide strained interfacial layer where the defect's bonds exhibit greater E_a values due to a higher oxide

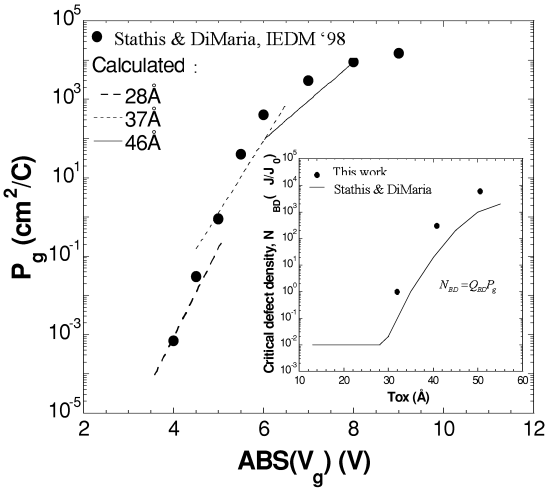

Fig. 9. Defect generation rate vs. gate bias calculated for different oxide thickness. Insert: critical defect density vs. oxide thickness.

density in this layer, which effectively reduces the length of the precursor defect bonds. Accordingly, the trap generation probability is greater in the case of gate injection due to a higher density of localized states in the strained interfacial layer (compared to the bulk oxide), leading to a higher probability of electron capture and subsequently, to lower Q_{bd} values for the same E_{ox} (Figs. 6 and 7).

5. Discussion

As suggested above, H_2 may react with the remaining dangling O bond after the breakage of the Si–O bond, thus stabilizing an E′ center. Hydrogen supply in the oxide is determined to a great extent by the anode hydrogen release process, which is controlled by the electron energy at the anode interface, and therefore by the anode bias V_g (the absolute majority of the injected electrons tunnel through the oxide without interacting with localized states). When electric stress is applied on a set of similar devices (NMOS or PMOS) manufactured within the same process (in particular, having the same substrate doping level, gate electrode, gate oxide growth process, etc.), the oxide field E_{ox} scales with the anode bias V_g in a pre-determined way, $E_{ox} \propto \lambda V_g$.

This will take place in all devices establishing a constant ratio (specific for the given device type/manufacturing process) between the number of broken bonds, depending on E_{ox} and the available hydrogen determined by V_g. In this case, one can correlate the oxide degradation/breakdown to the E_{ox} values. The ratio of the broken bonds to the available hydrogen, however, is unique for each device type/process: for instance, P- and N-MOS devices or devices with differently doped substrates/electrodes [36,37], have a different scaling factor λ. The observed correlation of the breakdown parameters to the V_g values [1,36] indicates that hydrogen release at the anode interface may be the limiting factor in the oxide trap generation process.

This model suggests that new defects are preferentially created in the vicinity of traps previously created during stress (or existing prior to the stress) due to the formation of additional localized states associated with the newly generated E′ centers. Indeed, the density of localized states increases when

more second nearest oxygen neighbors are missing/displaced [12]. According to the model proposed here, capture of the injected electrons by these localized states can result in the generation of the precursor breakdown defects (an elongated Si–O) and subsequent bonds breakage. Formation of additional defects near the existing one further increases the density of the gap states around that location in the oxide since a greater number of oxygen atoms will be affected by the displacements of their second nearest neighbors. This process leads to the formation of a defect cluster whose growth rate increases with its volume (Fig. 10). Thus, an initial structural defect plays the role of a nucleation center for the generation of defect clusters, which may form a continuous link through the oxide, eventually creating a conductive path. As a result, any defect in the bulk of the oxide (even such seemingly benign defect as a large neutral interstitial impurity atom), which affects the bond angles and/or bond lengths of the surrounding atoms and generates a significant density of localized states, may initiate the defect cluster formation.

The Si/SiO_2 interface, which is characterized by oxygen deficiency and higher compressive stress, is an inherently defective oxide region wherein the defect cluster growth most probably initiates, as shown in Fig. 11. In the case of a high quality, uniform interface, multiple defect clusters grow from the interface under the same starting conditions, and the 'winner' cluster will be defined by random

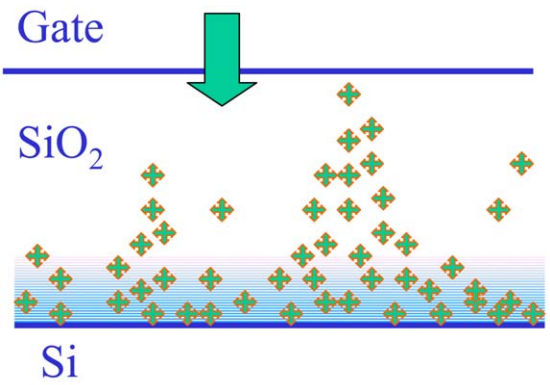

Fig. 11. Schematic of the trap cluster formation during electrical stress in the oxide. Shaded area represents the transitional oxygen deficient interfacial oxide region.

fluctuations in the defect generation process (due to variations in the oxide structure, charge flow, etc.). For devices with large gate areas and thick oxides these fluctuations are less relevant; hence, the process of growth of numerous defect clusters would be practically indistinguishable from the dynamics of random defect generation. The efficiency of the defect generation is expected to decrease away from the Si/SiO_2 interface due to a lower localized state density for a given injected electron energy in both substrate and gate injection cases.

The first cluster that spans across the oxide thickness during electrical stress sets the location of the breakdown region in the oxide, while the size of the cluster may determine the breakdown type, hard

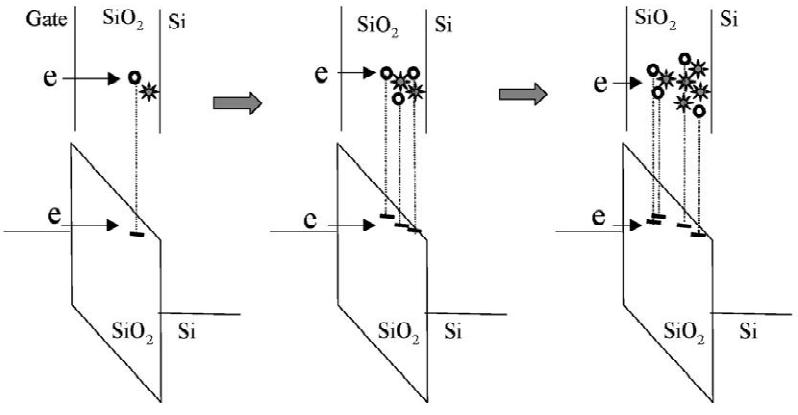

Fig. 10. Schematics of the defect cluster formation. Stars represent E′ centers and circles are their nearest-neighbor oxygen atoms. Electron capture by the localized states associated with these oxygen atoms can generate new E′ centers at the sites of the oxygen atoms.

or soft, depending on the cluster characteristic dimension (cross-section in the Si/SiO_2 plane). In thinner oxides, soft breakdown events are more probable since the defect cluster may connect the substrate and the gate before its characteristic dimension can sustain a high current causing hard breakdown. Under continued stress, the initial highly resistive conduction path gets more conductive due to the effective generation of new traps next to the already existing ones. Since the growth rate of the defect cluster is proportional to its size, the first conductive path, which is likely to correspond to the largest defect cluster, generates more traps nearby than other defect clusters in the given device, thus increasing the characteristic dimension of the initial conductive path (Fig. 11). This model suggests that the evolution of the initial soft breakdown path toward a hard breakdown is the *preferable* mechanism for thin oxide degradation as opposed to formation of additional soft breakdown paths. Such evolution of the oxide breakdown path has been observed experimentally [38].

How the presence of traps actually contributes to the conduction across the oxide film is still not clearly established. One may suggest the following scenario: formation of the initial percolation path across the oxide allows for only highly resistive electron transport, most probably by an electron hopping via the traps. This type of transport is characteristic for the soft breakdown when the leakage current increases insignificantly, its magnitude being unstable and characterized by high standard deviation. The initial percolation path could be transformed into a conductive path by the subsequent stress. The formation of a conduction path may be considered as a change of the local material properties from dielectric to conductor along the percolation path. From this standpoint, conduction features could be achieved by effectively 'doping' the dielectric with electrons by means of filling the electron traps. The overlap of the electron wavefunctions localized near the traps forms a 'conduction band', which is localized along the percolation path (Fig. 12). This overlap depends on the traps energy and density, temperature and applied voltage. Higher temperature/voltage increases delocalization of the wavefuction of the trapped electrons by increasing population of the excited vibrational states in the

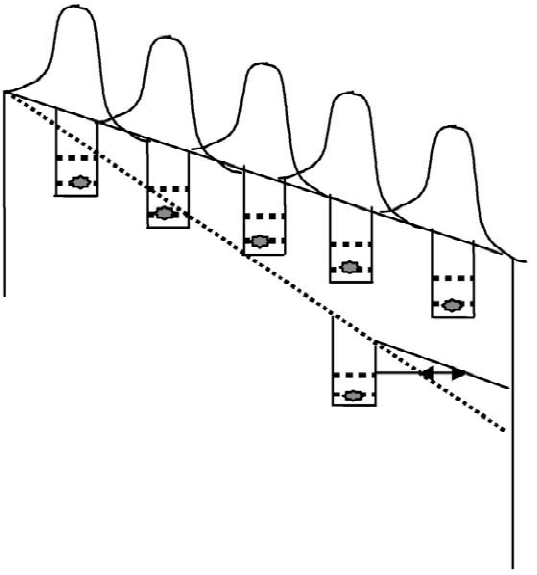

Fig. 12. Schematic of the conduction band formation along the percolation path in the oxide. Stars represent the trapped electrons, the broken lines correspond to the vibrational states in the energy well associated with the traps, and the solid lines are the electrons' wavefunctions. The arrow illustrates reduction of the trap energy barrier width under increased gate bias in comparison to the low-biased case (dotted line).

traps and reduces the energy barrier of each individual minimum, respectively (similar to the situation described by Fig. 5). As a result, an overlap of the wavefuctions of the electrons trapped in the adjacent minima increases with higher temperature/bias leading to lesser traps in the percolation path required to generate conduction. Such effective reduction of the critical trap density at elevated temperatures may be manifested in the observed deviation of the temperature dependence of the measured time-to-breakdown from the Arrhenius relation [39]. On the other hand, with the given generated trap density, a transition from a soft to a hard breakdown, which we suggest is caused by the formation of the localized conduction band along the percolation path, could be triggered by a small increase in the applied voltage. A change of the voltage across the dielectric determines the reduction of the trap's energy barrier height and width (Fig. 12), from which the delocalization and corresponding overlap of the trapped electron wavefuction depends exponentially.

Therefore, the formation of a conductive path requires both generation of electron traps (which takes place during high voltage stress) and filling of those traps (which also occurs at lower voltages). In the latter process, an electric field associated with the trapped electrons can influence subsequent electron trapping in the nearby traps [40]. In particular, the trap energy might be significantly reduced causing a 'random' electron de-trapping. It is reasonable to speculate that such complex trapping/de-trapping process may cause the stress current instability observed before and around a soft breakdown event. If trap filling is required for the transformation of the percolation path in the oxide into a conductive path, then a significant number of trapped electrons should be expected to remain in the traps after the breakdown. A study of the post-soft breakdown oxides using the conductive AFM technique does show negative charge located in the breakdown path [41].

Oxide irradiation [42] and hot hole injection experiments [5,6] show that holes, if indeed injected into the oxide during CVS, can potentially generate electron traps causing SILC and subsequent breakdown. It was suggested that holes break Si–Si bonds at oxygen vacancy defects, and may also 'cleave' highly strained Si–O–Si bonds at the SiO_2/Si interface, resulting in the formation of the positively charged E′ centers [43]. Holes can also activate E′ centers by hydrogen release from O_3≡Si–H defects [44]. For the case of hole generated E′ centers, a random distribution of the E′ centers in the film following the distribution of the oxygen vacancies or hydrogen defects should be expected. Also expected is the reduction of trap generation rate with the stress time due to a limited number of the pre-existing defects available within the hole diffusion distance from the anode interface, and different trap energies due to a positive charge or structural arrangements around the centers. As a result, a hole-induced dielectric breakdown should show critical defect density and temperature dependence different from those caused by electron capture by localized states. Such difference between the oxide degradation characteristics has been observed in HHE and CVS experiments [5,6]. We speculate that the CVS breakdown is associated with electron-induced traps; however, a contribution of hole-induced traps to SILC cannot be ruled out. Indeed, there are indications, based on the traps filling kinetics and temperature dependence of generation, that CVS may produce more than one type of trap [45]. Time dependence of the CVS generated SILC shows that it tends to saturate before a soft breakdown takes place [4]. Furthermore, SILC annealing experiments [3] point to essential differences in SILC- and SB-related traps, though both may be the E′-type centers. The observed SILC features are not inconsistent with the ones expected from SILC traps initiated by holes at pre-existing defect sites, such as oxygen vacancies [46] or hydrogen-related defects [44].

6. Summary

The proposed model describes a sequence of events leading to the formation of the E′ centers under electrical stress. Oxide structural imperfections, especially in the transitional layer at the SiO_2/Si interface induce localized states in the oxide band gap, which can capture injected electrons. Quantum-chemical calculations indicate that the electron capture significantly weakens the Si–O bond associated with the localized state. This bond can then be broken by an applied electric field/temperature (or with no field at all if the bond is additionally weakened by structural stress). The broken bond can be restored when the captured electron is released. However, molecular hydrogen (most probably released from the Si interface by the majority of the injected electrons, which did not interact with the localized states) may react with the dangling oxygen bond preventing the bond restoration and thus leading to a neutral E′ center formation. This model identifies the structural features in the oxide that may serve as defect precursors, as well as their formation mechanism, and suggests an explanation for the role of hydrogen in the breakdown process.

References

[1] J. Suehle, IEEE Trans. Electron Dev. 49 (2002) 958.
[2] IBM J. Res. Dev. 43(3) (1999).
[3] L. Pantisano, K.P. Cheung, IEEE Trans. Device Mater. Reliability 1 (2001) 109.

[4] P. Riess, G. Ghibaudo, G. Pananakakis, J. Appl. Phys. 87 (2000) 4626.
[5] E.M. Vogel, M.D. Edelstein, J.S. Suehle, J. Appl. Phys. 90 (2001) 1.
[6] W.D. Zhang et al., INFOS 2001 (2001) 169.
[7] P.M. Lenahan et al., Proc. IRPS-IEEE (2001) 150;
P.M. Lenahan, J.J. Mele, R.K. Lowry, D. Woodbury, J. Non-Cryst. Solids 266 (2000) 835.
[8] J. McPherson et al., J. Appl. Phys. 88 (2000) 5351.
[9] D.J. DiMaria, J.W. Stasiak, J. Appl. Phys. 65 (1989) 2342.
[10] M.A. Alam et al., The physics and chemistry of SiO_2/Si interface, ECS Proc. 2000–2 (2000) 295.
[11] G. Bersuker, IEEE-IRPS Tutorial 2002, Adv. Reliability Top. (2002) 224.
[12] J.B. Neaton et al., Phys. Rev. Lett. 85 (2000) 1298.
[13] A. Pasquarello, M.S. Hybertsen, R. Car, Nature 396 (1998) 58.
[14] T. Yamasaki, C. Kaneta, T. Uchiyama, T. Uda, K. Terakura, The physics and chemistry of SiO_2/Si interface, ECS Proc. 2000–2 (2000) 295.
[15] G. Bersuker, Y. Jeon, H.R. Huff, Microelectronics Reliability 41 (2001) 1923.
[16] G. Bersuker, A. Korkin, Y. Jeon, H.R. Huff, Appl. Phys. Lett. 80 (2002) 832.
[17] A. Korkin, G.I. Bersuker, H.R. Huff, Comput. Mater. Sci. 24 (2002) 223–228.
[18] P. Hohenberg, W. Kohn, Phys. Rev. B 136 (1964) 864;
S.H. Vosko, L. Wilk, M. Nusair, Can. J. Phys. 58 (1980) 1200;
A.D. Becke, Phys. Rev. A38 (1988) 3098;
C. Lee, W Yang, R.G. Parr, Phys. Rev. B37 (1988) 785;
M. Head-Gordon, J.A. Pople, M.J. Frisch, Chem. Phys. Lett. 153 (1988) 503.
[19] M.J. Frisch et al., Gaussian 98, rev A.6, Gaussian, Inc, Pittsburgh, PA, 1998.
[20] Y. Harada, K. Eriguchi, M. Niwa, T. Watanabe, I. Ohdomari, Jpn. J. Appl. Phys. 39 (2000);;
W. Mizubayashi, Y. Yoshida, S. Miyazaki, M. Hirose, VLSI Tech. Digest (2001) 95.
[21] J.D. DiMaria, J. Appl. Phys. 87 (2000) 8707.
[22] G. Pacchioni, Defects in SiO_2 and Related Dielectrics: Science and Technology, 2000, p. 161.
[23] D.M. Ceperley, B.J. Alder, Phys. Rev. Lett. 45 (1980) 566;
J.P. Perdew, A. Zunger, Phys. Rev. B 23 (1981) 5048.
[24] P. Hohenberg, W. Kohn, Phys. Rev. 136 (1964) B864;
W. Kohn, L.J. Sham, Phys. Rev. 140 (1965) A1133.
[25] J.M. Soler, E. Artacho, J.D. Gale, A. Garcia, J. Junquera, J. Phys.: Condens. Matter 14 (2002) 2745.
[26] M.P. Teter, M.C. Payne, D.C. Allen, Phys. Rev. B 40 (1989) 12255.
[27] R.P. Feynman, Phys. Rev. 56 (1939) 340;
H. Hellmann, Einfuhrung in die Quantumchemie, Deutiche, Leipzig, 1937.
[28] N. Troullier, J.L. Martins, Phys. Rev. B 43 (1991) 1993.
[29] J.H. McPherson, H.C. Mogul, IEEE-IRPS Proc. (1998) 47.
[30] R. Degraeve, G. Groeseneken, R. Bellens, M. Depas, H.E. Maes, IEDM Tech. Digest (1995) 863.
[31] D.J. DiMaria, Microelectronic Eng. 36 (1997) 317.
[32] M. Kimura, IEEE-IRPS Proc. (1997) 190.
[33] K.F. Schuegraf, C.C. King, C. Hu, VLSI Tech. Digest (1992) 18.
[34] J.H. Stathis, D.J. DiMaria, IEDM Tech. Digest (1998) 167.
[35] T. Watanabe, I. Ohdomari, The physics and chemistry of SiO_2/Si interface, ECS Proc. 2000–2 (2000) 319.
[36] P.E. Nicollian, W.R. Hunter, J.C. Hu, IEEE-IRPS (2000) 7.
[37] J.M. McKenna, E.Y. Wu, S.-H. Lo, IEEE-IRPS Proc. (2000) 16.
[38] F. Monsieur et al., IEEE Integrated Reliability Workshop Final Report, Lake Tahoe, 2002.
[39] R. Degraeve et al., VLSI Tech. Digest (1999) 59.
[40] V.A. Gritsenko et al., Phys. Rev. Lett. 81 (1998) 1054.
[41] M. Porti, M. Nafria, M.C. Blum, X. Aymerich, S. Sadewasser, Appl. Phys. Lett 8 (2002) 3615.
[42] A. Scarpa et al., Microelectronics Reliability 40 (2000) 57.
[43] T.P. Ma, P.V. Dressendorfer, Ionizing Radiation Effects in MOS Devices and Circuits, NY, 1989.
[44] V.V. Afanas'ev, A. Stesmans, Mater. Sci. Semicond. Processing 4 (2001) 149.
[45] W.D. Zhang et al., Abstracts of the 33rd IEEE Semicond. Interface Specialists Conference, San Diego, 2002.
[46] A. Yokozawa et al., IEDM Tech. Digest (1997) 703.